JOURNAL OF GUIDANCE, CONTROL, AND DYNAMICS
Vol. 20, No. 5, September–October 1997

Approximate Decoupling Flight Control Design with Output Feedback

S. Park* and M. G. Nagati†
Wichita State University, Wichita, Kansas 67260-0044

The problem of approximate decoupling of nonlinear systems by output feedback is considered. The structure of the controller is high-gain proportional plus integral. Linearization of the nonlinear closed-loop equations results in the standard singular perturbation form. Based on the singular perturbation concept, a control law is found that accomplishes approximate decoupling with stability for nonlinear systems. Application of the proposed design scheme to the full six-degree-of-freedom nonlinear aircraft dynamics model is presented, demonstrating its validity.

I. Introduction

A SYSTEM is said to be decoupled if each component of the output depends only on the corresponding component of the input. The problem of decoupling a multivariable system has been extensively treated in the literature in the past 30 years. The necessary and sufficient conditions were developed for linear[1,2] and nonlinear[3–6] systems. However, no systematic procedures for the controller design were considered.

Nonlinear system controller design is typically approached by linearizing the system about a nominal operating point and applying linear system design methods. This will provide a linear control law that yields approximate noninteracting control and satisfy design objectives in the neighborhood of the constant operating point. For the purpose of this work, the design objectives for this highly coupled system of flight dynamics are to closely track individual desired outputs, with zero steady-state response from others. However, the problem of computing the decoupling feedback control laws for a nonlinear system is quite difficult.

Approximate decoupling control for nonlinear systems is based on singular perturbation concepts. The structure of controller is high-gain output feedback with proportional plus integral (PI) control. It will be shown that the linearization of nonlinear closed-loop system about the nominal operating point yields the standard singular perturbation equation form when a scalar gain weighting $g \to \infty$. Then, the singular perturbation concept, i.e., necessary and sufficient conditions, is utilized to find a decoupling control law.

This approach is a new, conceptually simple, but practically useful design method for approximate noninteracting control law design with stability for nonlinear systems. The results developed are easy to follow and are easily applicable to aircraft control decoupling problems. This paper introduces the application of this design method to approximate noninteracting flight control system design.

II. Theoretical Development

We assume that the nonlinear system to be controlled is represented by

$$\dot{\boldsymbol{X}}(t) = \boldsymbol{f}[(\boldsymbol{X}(t), \boldsymbol{U}(t)], \qquad \boldsymbol{Y}(t) = C\boldsymbol{X}(t) \tag{1}$$

$\boldsymbol{X} \in \Re^n$ is the state, $\boldsymbol{U} \in \Re^m$ is the control, and $\boldsymbol{Y} \in \Re^m$ is the output. $C \in \Re^{m \times n}$ is the control matrix. The vector function $\boldsymbol{f}(\boldsymbol{X}, \boldsymbol{U})$ is assumed to be continuously differentiable in a neighborhood of the respective origins. Assuming that the structure of controller is output feedback with PI control,

$$\boldsymbol{U}(t) = g\left[K_P\boldsymbol{e}(t) + K_I\int_0^t \boldsymbol{e}(t)\,\mathrm{d}t\right] \tag{2}$$

$$\boldsymbol{e}(t) = \boldsymbol{V}(t) - \boldsymbol{Y}(t) \tag{3}$$

where g is the positive scalar gain parameter; $\boldsymbol{e}(t)$ is the $(m \times 1)$ error vector; $\boldsymbol{V}(t)$ is the $(m \times 1)$ constant reference signal, i.e., desired output command; K_P is the $(m \times m)$ proportional error controller matrix; and K_I is the $m \times m$ integral error controller matrix.

Applying the control law into the plant (1), we obtain the nonlinear closed loop as follows. By differentiating Eq. (2), we have

$$\dot{\boldsymbol{U}} = g[K_P\dot{\boldsymbol{e}} + K_I\boldsymbol{e}] \tag{4}$$

Because $\boldsymbol{e} = \boldsymbol{V} - \boldsymbol{Y}$ and $\boldsymbol{Y} = C\boldsymbol{X}$,

$$\dot{\boldsymbol{U}} = g[-K_PC\dot{\boldsymbol{X}} + K_I(\boldsymbol{V} - C\boldsymbol{X})] \tag{5}$$

Equation (1) is substituted into Eq. (5) to obtain

$$\dot{\boldsymbol{U}} = -g[K_PC\boldsymbol{f}(\boldsymbol{X}, \boldsymbol{U}) + K_IC\boldsymbol{X}] + gK_I\boldsymbol{V} \tag{6}$$

Augmenting the state equation (1) with Eq. (6), we obtain the closed-loop equations

$$\begin{pmatrix} \dot{\boldsymbol{X}} \\ \dot{\boldsymbol{U}} \end{pmatrix} = \begin{pmatrix} \boldsymbol{f}(\boldsymbol{X}, \boldsymbol{U}) \\ -g[K_PC\boldsymbol{f}(\boldsymbol{X}, \boldsymbol{U}) + K_IC\boldsymbol{X}] \end{pmatrix} + \begin{pmatrix} 0 \\ gK_I \end{pmatrix}\boldsymbol{V} \tag{7}$$

$$\boldsymbol{Y}_{\mathrm{cl}} = \begin{pmatrix} C & 0 \\ 0 & I_m \end{pmatrix}\begin{pmatrix} \boldsymbol{X} \\ \boldsymbol{U} \end{pmatrix} \tag{8}$$

The nonlinear closed-loop block diagram for the output PI control is shown in Fig. 1. From Eq. (7), we notice that it is a two-time-scale system in which the plant state $\boldsymbol{X}$ is the slow state and the control $\boldsymbol{U}$ is the fast state, if g is sufficiently large.

To decouple the input–output behavior of the nonlinear closed-loop system, one would like to design $\boldsymbol{U}$, i.e., a control law, such that

$$\lim_{t \to \infty} \dot{\boldsymbol{X}}(t) \to 0$$

for stability and

$$\lim_{t \to \infty} \boldsymbol{Y}(t) \to \boldsymbol{Y}_{\mathrm{ref}}$$

for zero steady-state errors. This is referred to as asymptotic decoupling. This means that there is a one-to-one correspondence between any ith output vector and the corresponding ith input control. It is a reasonable assumption that the choice of K_P and K_I will ensure the asymptotic stability of the nonlinear closed-loop system.

Presented as Paper 93-3880 at the AIAA Guidance, Navigation, and Control Conference, Monterey, CA, Aug. 9–11, 1993; received June 8, 1995; revision received June 1, 1997; accepted for publication June 11, 1997.

*Graduate Student, Department of Aerospace Engineering; currently Senior Research Engineer, Research and Development Division, Hyundai Space and Aircraft Co., Ltd., 140-2 Gye-Dong, Chongro-Ku, Seoul, Republic of Korea.

†Associate Professor, Department of Aerospace Engineering. Associate Fellow AIAA.

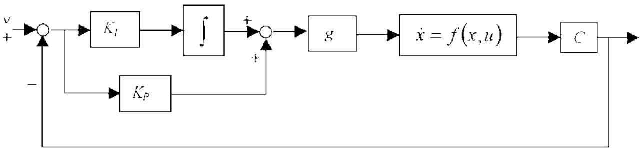

Fig. 1 Nonlinear closed-loop block diagram for the output feedback with PI control.

Then, the problem is to choose the output feedback gains K_P and K_I to achieve the asymptotic stability of the zero-input response of Eq. (7).

A. Singular Perturbation Form Formulation

A typical way to approach this problem is to linearize the plant at a nominal constant operating point and apply the linear system theory. Then, linearization of Eq. (7) about the constant operating points yields

$$\begin{pmatrix}\dot{x}\\ \dot{u}\end{pmatrix} = \begin{pmatrix} A & B \\ -g[K_P CA + K_I C] & -gK_P CB\end{pmatrix}\begin{pmatrix}x\\ u\end{pmatrix} + \begin{pmatrix}0\\ gK_I\end{pmatrix} v \tag{9}$$

$$y_{\mathrm{cl}} = \begin{pmatrix} C & 0\\ 0 & I_m\end{pmatrix}\begin{pmatrix}x\\ u\end{pmatrix} \tag{10}$$

where

$$A = \frac{\partial f_1(X_0, U_0)}{\partial X}, \qquad B = \frac{\partial f_1(X_0, U_0)}{\partial U} \tag{11}$$

and

$$f_1 = f(X_0, U_0)$$
$$f_2 = h(X_0, U_0, V_0) = -g[K_P C f(X_0, U_0) + K_I C X_0] + gK_I V_0 \tag{12}$$

Note that $x(t) = X(t) - X_0$, $u(t) = U(t) - U_0$, $v = V - V_0$, and $y(t) = Y(t) - Y_0$ are the perturbation variables. Here, the subscript 0 indicates the nominal value. $A \in \Re^{n\times n}$ is the state matrix, $B \in \Re^{n\times m}$ is the control matrix, and $C \in \Re^{m\times n}$ is the output matrix.

We can obtain the same result, i.e., Eq. (9), by augmenting the linear time invariant system with the proposed controller. The decoupling synthesis procedure presented coincides with linear systems design in Ref. 7. The general approach for this method is described as follows.

From Eqs. (9) and (10), the linearized state and output equations are represented by

$$\dot{x}(t) = Ax(t) + Bu(t), \qquad y(t) = Cx(t) \tag{13}$$

Note that the input and output have the same dimension so as to satisfy the design objective.

Next, we write the state and output equations (13) in the form

$$\begin{pmatrix}\dot{x}_1(t)\\ \dot{x}_2(t)\end{pmatrix} = \begin{pmatrix}A_{11} & A_{12}\\ A_{21} & A_{22}\end{pmatrix}\begin{pmatrix}x_1(t)\\ x_2(t)\end{pmatrix} + \begin{pmatrix}B_1\\ B_2\end{pmatrix} u(t) \tag{14}$$

$$y(t) = [C_1 \quad C_2]\begin{pmatrix}x_1(t)\\ x_2(t)\end{pmatrix} \tag{15}$$

where B_2 is a square nonsingular matrix and $x_1 \in \Re^{n-m}$, $x_2 \in \Re^m$, $u \in \Re^m$, and $y \in \Re^m$. The dimensions of the matrices follow.

From Eq. (9), the results of singular perturbation theory can be applied by letting the perturbation parameter ε be the reciprocal of the forward path gain g, i.e., $\varepsilon \to 0$ as $g \to \infty$. Letting, $\varepsilon = 1/g$, we have

$$\begin{aligned}\varepsilon\dot{u} &= -[K_P CA + K_I C]x - K_P CBu + K_I v\\ &= -[K_P CA + K_I C]x - K_P[C_1 B_1 + C_2 B_2]u + K_I v\end{aligned} \tag{16}$$

Substituting Eq. (16) into Eq. (9), we obtain a closed-loop equation that has the standard singular perturbation equation form

$$\begin{pmatrix}\dot{x}\\ \varepsilon\dot{u}\end{pmatrix} = \begin{pmatrix}A_1 & A_2\\ A_3 & A_4\end{pmatrix}\begin{pmatrix}x\\ u\end{pmatrix} + \begin{pmatrix}D_1\\ D_2\end{pmatrix} v$$
$$y_{\mathrm{cl}} = \begin{pmatrix}C & 0\\ 0 & I_m\end{pmatrix}\begin{pmatrix}x\\ u\end{pmatrix} = [H_1 \quad H_2]\begin{pmatrix}x\\ u\end{pmatrix} \tag{17}$$

which can be analyzed by methods such as in Refs. 8 and 9. In singular perturbation theory, it is assumed that matrix A_4 is nonsingular and stable (has eigenvalues with negative real parts) and D_2 is nonsingular. With singular perturbation theory,[7,10] the asymptotic properties of the closed-loop transfer function can be examined to determine the location of the closed-loop poles, as the forward path gain g becomes increasingly large.

Based on Eq. (9), the values of g, K_P, and K_I are chosen such that the eigenvalues of the closed-loop equation are in the left-half plane. The controller matrices K_P and K_I are computed by using the given assumptions, i.e., A_4 is stable and nonsingular. This can be achieved by using the first Markov parameter C_2B_2 of the plant as their basis [Eq. (16)]. However, this is possible if the matrix pair (A, B) is controllable.

Once the plant is in the required form [Eqs. (14) and (15)], its first Markov parameter, i.e., C_2B_2, is determined. If C_2 is rank deficient, the plant is called irregular. Because B_2 is constrained to have full rank, C_2 must be augmented to make it full rank. This is accomplished by introducing a measurement matrix M (Refs. 11 and 12). The trackers examined in this work are irregular, requiring a measurement matrix M.

For an irregular system, we now define the output measurements $w(t)$, which track the command inputs $v(t)$, as

$$w(t) = [F_1 \quad F_2]\begin{pmatrix}x_1(t)\\ x_2(t)\end{pmatrix} = [C_1 + MA_{11} \quad C_2 + MA_{12}]\begin{pmatrix}x_1(t)\\ x_2(t)\end{pmatrix} \tag{18}$$

where M is the extra plant measurement matrix (see Fig. 2). From Eq. (18), M is $m\times(n-m)$, F_1 is $m\times(n-m)$, and F_2 is $m\times m$. The new first Markov parameter is F_2B_2. This requires F_2 to be full rank so that F_2B_2 has full rank, i.e., rank$[F_2]$ = rank$[C_2 + MA_{12}] = m$. In addition, we choose a sparse measurement matrix to keep the coupling between the output variables as low as possible. From Eq. (3), we redefine the error vector $e(t)$ as

$$e(t) = v(t) - w(t) \tag{19}$$

To achieve the noninteraction, it is desired that the control input vector $u(t)$ cause the output vector $y(t)$ to track any constant command input vector $v(t)$, i.e.,

$$\lim_{t\to\infty} e(t) = \lim_{t\to\infty}[v - y(t)] = 0 \tag{20}$$

The steady-state value of $w(t)$ is

$$\begin{aligned}\lim_{t\to\infty} w(t) &= \lim_{t\to\infty}[F_1x_1(t) + F_2x_2(t)]\\ &= \lim_{t\to\infty}[C_1x_1(t) + C_2x_2(t) + M\dot{x}_1(t)]\end{aligned} \tag{21}$$

From the state equations (14), it is evident that for a stable system

$$\lim_{t\to\infty} w(t) = \lim_{t\to\infty}[y(t) + MB_1u(t)] \tag{22}$$

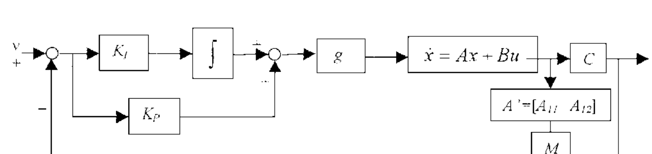

Fig. 2 Block diagram of the linear irregular tracking system.

If MB_2 is negligible, the steady-state value of $\boldsymbol{w}$ approaches $\boldsymbol{y}$. Thus, from Eq. (19), we can also assume that

$$\lim_{t\to\infty} \boldsymbol{e}(t) = \lim_{t\to\infty} [\boldsymbol{v} - \boldsymbol{w}(t)] \approx 0 \tag{23}$$

This result clearly indicates that noninteraction is achievable. Thus, for the irregular system, the closed-loop equations become

$$\begin{pmatrix} \dot{\boldsymbol{x}} \\ \dot{\boldsymbol{u}} \end{pmatrix} = \begin{pmatrix} A & B \\ -g[K_P FA + K_I F] & -gK_P FB \end{pmatrix} \begin{pmatrix} \boldsymbol{x} \\ \boldsymbol{u} \end{pmatrix} + \begin{pmatrix} 0 \\ gK_I \end{pmatrix} \boldsymbol{v} \tag{24}$$

$$\boldsymbol{y}_{\text{cl}} = \begin{pmatrix} C & 0 \\ 0 & I_m \end{pmatrix} \begin{pmatrix} \boldsymbol{x} \\ \boldsymbol{u} \end{pmatrix} \tag{25}$$

From Eq. (24), we note that $FB = [F_1 \ \ F_2][B_1 \ \ B_2]^T$. Thus, by rearranging Eq. (24), we obtain the closed-loop equations

$$\begin{pmatrix} \dot{\boldsymbol{x}} \\ \dot{\boldsymbol{u}} \end{pmatrix} = \begin{pmatrix} A & B \\ -g[K_P FA + K_I F] & -gK_P[F_1B_1 + F_2B_2] \end{pmatrix} \begin{pmatrix} \boldsymbol{x} \\ \boldsymbol{u} \end{pmatrix} + \begin{pmatrix} 0 \\ gK_I \end{pmatrix} \boldsymbol{v} \tag{26}$$

$$\boldsymbol{y}_{\text{cl}} = \begin{pmatrix} C & 0 \\ 0 & I_m \end{pmatrix} \begin{pmatrix} \boldsymbol{x} \\ \boldsymbol{u} \end{pmatrix} \tag{27}$$

B. Finding the Control Gains K_P and K_I

As mentioned earlier, finding K_P is based on the given assumptions, i.e., singular perturbation concepts, that A_4 is nonsingular and stable. The eigenvalues of A_4 are large compared to those of A when ε is sufficiently small. For the irregular system, comparing Eqs. (17) and (26), we note that $A_4 = K_P FB$. Thus, without loss of generality,

$$K_P[F_1B_1 + F_2B_2] = \Sigma = \text{diag}(q_1, q_2, \ldots, q_m) \tag{28}$$

where q_i are positive real numbers. By selecting appropriate values for q_i, the elements of K_P can then be determined from

$$K_P = \Sigma(F_1B_1 + F_2B_2)^{-1} \tag{29}$$

If F_1B_1 is negligible, we can rewrite Eq. (29) as

$$K_P = \Sigma(F_2B_2)^{-1} \tag{30}$$

The integral gain K_I may be chosen as a positive multiple of proportional gain K_P

$$K_I = L_0 K_P \tag{31}$$

where $L_0 = \text{diag}(l_1, l_2, \ldots, l_m)$. Depending on the baseline plant model, the range of l_i can be chosen between 1 and 3.

Thus, having specified the design parameters, i.e., L_0 and Σ, and choosing the sparse measurement matrix M, so that $\text{rank}(F_2) = \text{rank}(C_2 + MA_{12}) = m$, we can find K_P and K_I. Then, by choosing the gain parameter g, the closed-loop matrices [Eq. (26)], can be calculated. As the gain parameter g increases, the poles of the closed loop approach their asymptotic values, and the closed-loop behavior becomes increasingly noninteracting. Using Eq. (26), the closed-loop eigenvalues for the entire system and the time histories of all of the states and outputs can be calculated.

III. Design Example

This section illustrates the use of the foregoing theory to design a robust multivariable approximate decoupling controller for a nonlinear system. The plant model for this example is based on the business jet aircraft model given in Ref. 13. The flight condition considered is the power approach condition at sea level. In this example, the linearized total aircraft plant model[7] for a business jet performing straight and level nonaccelerated flight for these flight conditions contains eight states and four inputs.

The linearized equations of motion of the aircraft are described by

$$\dot{\boldsymbol{x}} = A\boldsymbol{x} + B\boldsymbol{u} \tag{32}$$

where

$$A = \begin{pmatrix} 0.000 & 0.000 & 0.000 & 0.000 & 0.000 & 1.000 & 0.000 & 0.000 \\ 0.000 & 0.000 & 0.000 & 0.000 & 0.000 & 0.000 & 1.000 & 0.000 \\ 0.000 & 0.000 & -0.608 & 0.000 & -0.002 & 0.987 & 0.000 & 0.000 \\ 0.000 & 0.189 & 0.000 & -0.084 & 0.000 & 0.000 & 0.000 & -0.995 \\ -32.2 & 0.000 & 11.354 & 0.000 & -0.059 & 0.000 & 0.000 & 0.000 \\ 0.000 & 0.000 & -1.857 & 0.000 & 0.001 & -1.179 & 0.000 & 0.000 \\ 0.000 & 0.000 & 0.000 & -1.643 & 0.000 & 0.000 & -0.377 & 0.429 \\ 0.000 & 0.000 & 0.000 & 0.815 & 0.000 & 0.000 & -0.084 & -0.138 \end{pmatrix}, \qquad B = \begin{pmatrix} 0.000 & 0.000 & 0.000 & 0.000 \\ 0.000 & 0.000 & 0.000 & 0.000 \\ -0.046 & 0.000 & 0.000 & 0.000 \\ 0.000 & 0.000 & 0.000 & 0.016 \\ 0.000 & 0.076 & 0.000 & 0.000 \\ -3.031 & 0.000 & 0.000 & 0.000 \\ 0.000 & 0.000 & 1.427 & 0.124 \\ 0.000 & 0.000 & -0.250 & -0.419 \end{pmatrix}$$

The state vector is $\boldsymbol{x} = [\theta, \phi, \alpha, \beta, u, q, p, r]^T$, where

θ = perturbed pitch angle, rad
ϕ = perturbed roll angle, rad
α = perturbed angle of attack, rad
β = perturbed sideslip angle, rad
u = perturbed forward velocity, ft/s
q = perturbed pitch rate, rad/s
p = perturbed roll rate, rad/s
r = perturbed yaw rate, rad/s

The control vector is $\boldsymbol{u} = [\delta_e, \delta_T, \delta_a, \delta_r]^T$, where

δ_e = elevator deflection, rad
δ_T = thrust, lb
δ_a = aileron deflection, rad
δ_r = rudder deflection, rad

Note that A and B are already in the required forms, i.e., Eq. (14),

$$A = \begin{pmatrix} A_{11} & A_{12} \\ A_{21} & A_{22} \end{pmatrix}, \qquad B = \begin{pmatrix} B_1 \\ B_2 \end{pmatrix}$$

where B_2 is a square nonsingular matrix.

Because the aircraft model has four controls, four plant outputs, i.e., two longitudinal mode outputs and two lateral mode outputs, can be controlled. Various combinations of four outputs are possible.

A. Linear Control Law Design

The eigenvalues of the open-loop system from matrix A are

$$\text{longitudinal modes} = \begin{pmatrix} -0.906 \pm 1.319j \\ -0.017 \pm 0.237j \end{pmatrix} \tag{33}$$

$$\text{lateral modes} = \begin{pmatrix} 0.061 \pm 1.024j \\ -0.751 \\ 0.030 \end{pmatrix} \tag{34}$$

We note that the aircraft dynamics are unstable in the lateral modes, i.e., spiral and Dutch roll mode. In this example, four maneuvers are presented: climb, speedup, coordinated turn, and level

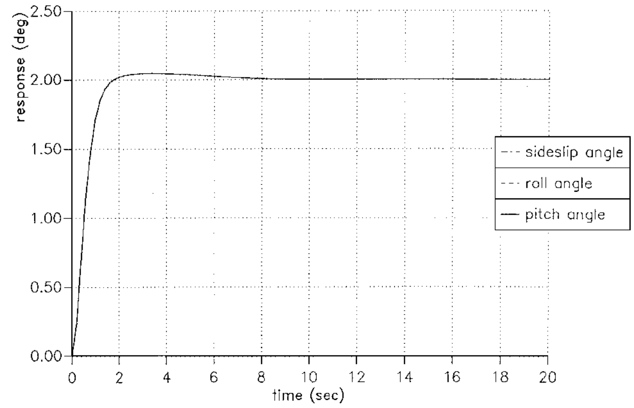

a) Time responses

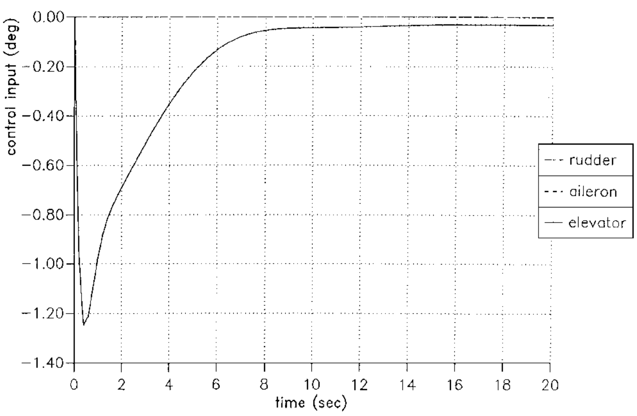

b) Control histories

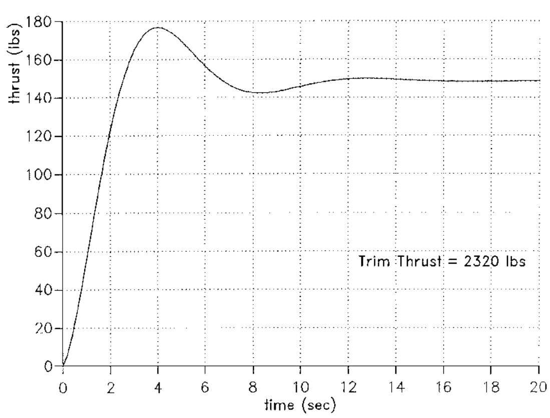

c) Thrust history

Fig. 3 Straight climb demand.

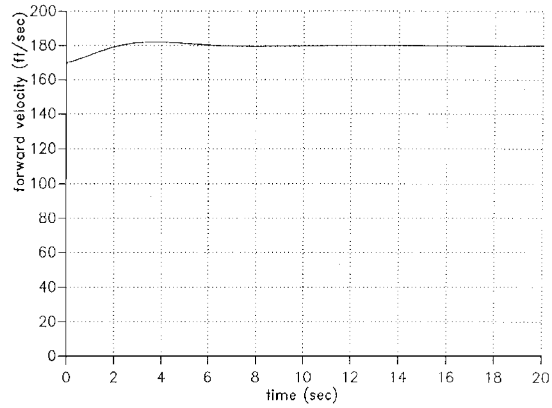

a) Forward velocity response

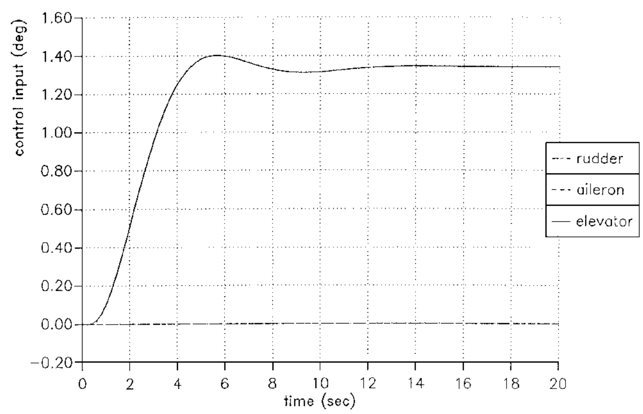

b) Control histories

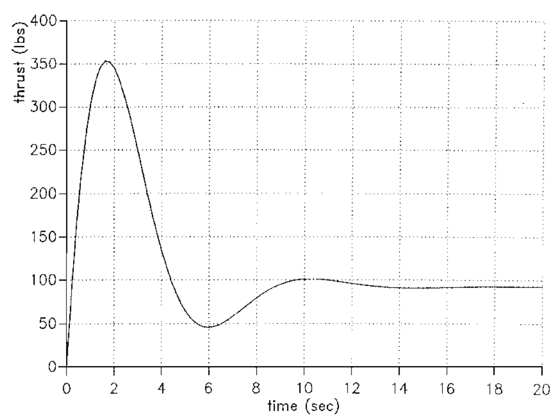

c) Thrust history

Fig. 4 Speed demand.

skidding. Therefore, the output vector is $\boldsymbol{y} = [\theta, \boldsymbol{u}, \phi, \beta]^T$, and the output matrix is

$$C = [C_1 \quad C_2] = \begin{pmatrix} 1 & 0 & 0 & 0 & 0 & 0 & 0 & 0 \\ 0 & 0 & 0 & 0 & 1 & 0 & 0 & 0 \\ 0 & 1 & 0 & 0 & 0 & 0 & 0 & 0 \\ 0 & 0 & 0 & 1 & 0 & 0 & 0 & 0 \end{pmatrix} \tag{35}$$

From Eq. (35), we note that C_2 has rank deficiency. Thus, this system requires the measurement matrix M. Because we have the eight state variables and four controls, the measurement matrix is 4×4 matrix. Because $F_2 = C_2 + MA_{12}$, we obtain, after some rounding off,

$$F_2 = \begin{pmatrix} 0 & m_{11} + 0.99m_{13} & m_{12} & -m_{14} \\ 1 & m_{21} + 0.99m_{23} & m_{22} & -m_{24} \\ 0 & m_{31} + 0.99m_{33} & m_{32} & -m_{34} \\ 0 & m_{41} + 0.99m_{43} & m_{42} & -m_{44} \end{pmatrix} \tag{36}$$

We choose m_{11}, m_{32}, and m_{44}, so that F_2 is a full rank matrix. Note that the measurement matrix is chosen to be the sparest matrix to avoid coupling between the output variables.

The following design parameters are used:

$$g = 30, \qquad L_0 = \text{diag}(2, 2, 2, 2), \qquad \Sigma = \text{diag}(1, 1, 1, 1) \tag{37}$$

$$M = \begin{pmatrix} 0.40 & 0.00 & 0.00 & 0.00 \\ 0.00 & 0.00 & 0.00 & 0.00 \\ 0.00 & 0.00 & 0.00 & 0.00 \\ 0.00 & 0.00 & 0.00 & 0.10 \end{pmatrix} \tag{38}$$

which give

$$F_2B_2 = \begin{pmatrix} -1.212 & 0.000 & 0.000 & 0.000 \\ 0.000 & 0.076 & 0.000 & 0.000 \\ 0.000 & 0.000 & 0.143 & 0.012 \\ 0.000 & 0.000 & 0.025 & 0.042 \end{pmatrix} \tag{39}$$

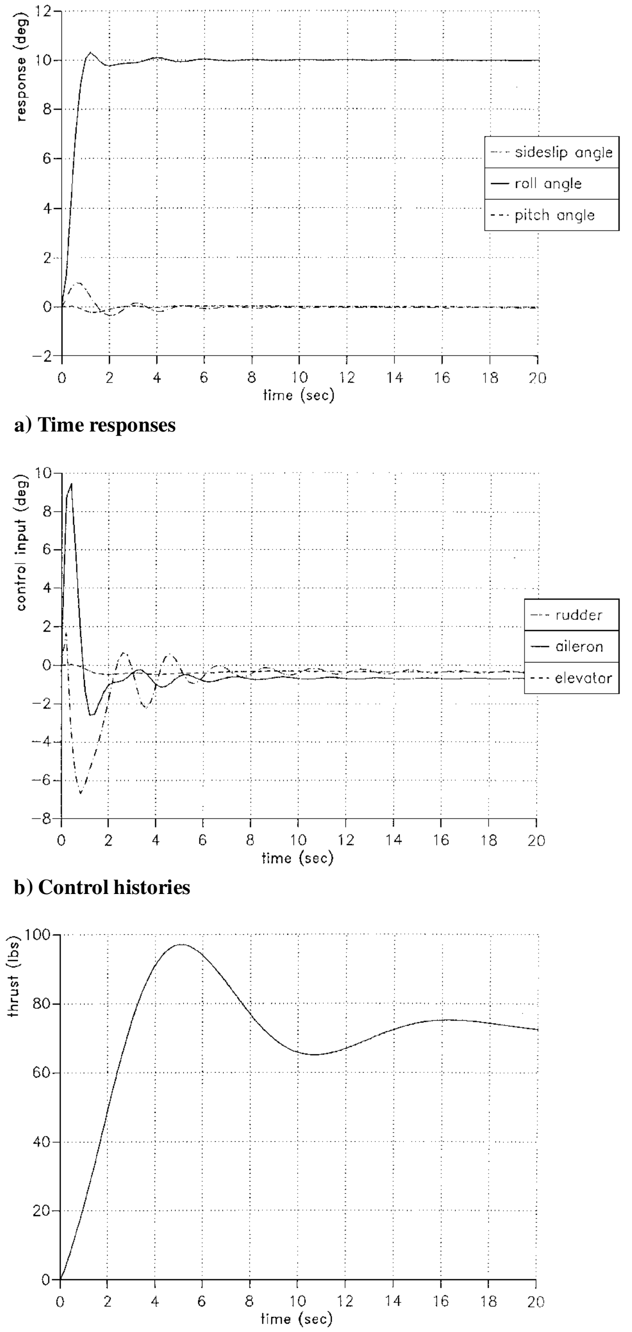

a) Time responses

b) Control histories

c) Thrust history

Fig. 5 Coordinated turn demand.

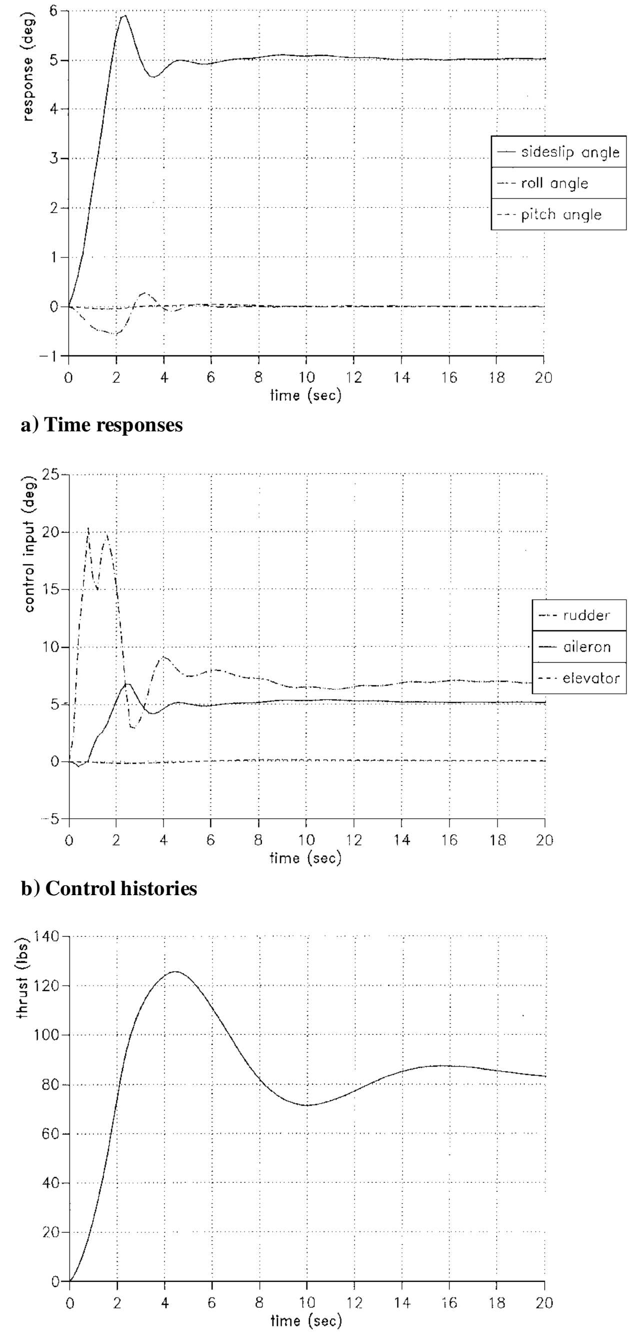

a) Time responses

b) Control histories

c) Thrust history

Fig. 6 Level skidding demand.

$$K_P = \begin{pmatrix} -0.825 & 0.000 & 0.000 & 0.000 \\ 0.000 & 13.158 & 0.000 & 0.000 \\ 0.000 & 0.000 & 7.393 & -2.198 \\ 0.000 & 0.000 & -4.401 & 25.269 \end{pmatrix}$$

$$K_I = L_0 K_P = 2K_P \tag{40}$$

Substituting these results, i.e., K_I, K_P, F, and g, and A and B into Eq. (26), the closed-loop system is obtained. The closed-loop eigenvalues are $\{-26.2013, -27.9084, -0.5869, -3.2716, -1.7260, -2.1518, -30.1512, -14.2454 \pm 10.0586j, -10.1371, -1.9764, -1.9604\}$.

B. Simulation

To test the performance of the design method, the designed linear output feedback PI controller is implemented on the six-degree-of-freedom nonlinear aircraft equations of motion. This is to see whether a control system designed by the proposed control system synthesis method will be physically realizable.

C. Simulation Results

In this example, four maneuvers for the power approach at sea level flight condition are presented: climb, speedup, coordinated turn, and level skidding.

The control vector is $\boldsymbol{u} = [\delta_e, \delta_T, \delta_a, \delta_r]^T$, and the output vector is $\boldsymbol{y} = [\theta, u, \phi, \beta]^T$.

The resulting controller gains, i.e., K_P and K_I, are implemented to the nonlinear closed-loop Eq. (8). The nonlinear closed-loop equations are integrated using the second-order Runge–Kutta method, with the step size $h = 0.02$. Because of the uncertainty in nonlinear systems, the constant parameter $g = 3$ is used.

Figures 3–7 are the time histories of the nonlinear closed-loop system simulation with the linear compensator. In general, these results are similar to the linear system responses. In Fig. 3a, a change of pitch angle from 0 to 2 deg is commanded. It can be seen that

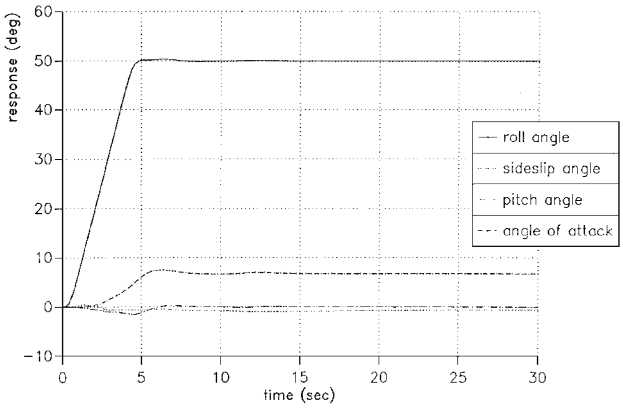

a) Time responses

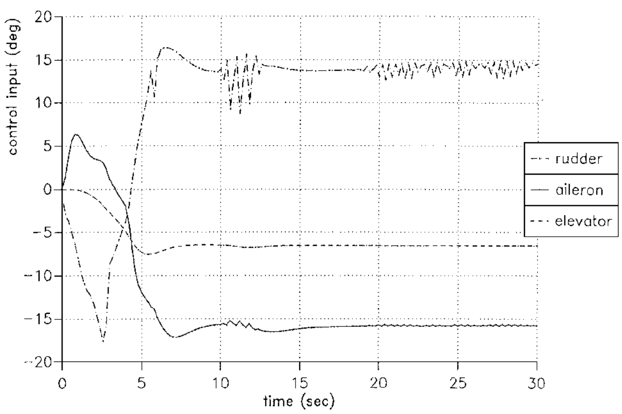

b) Control histories

Fig. 7 Coordinated turn demand.

coupling between pitch angle and speed is very small. Figure 4a shows the velocity response for the forward velocity demand from 170 to 180 ft/s. Again, pitch angle coupling is very small. For both cases, coupling between the longitudinal and lateral axes is absent, and the responses are smooth.

Figure 5a shows the bank angle demand from 0 to 10 deg. In Fig. 6a, a change of sideslip angle from 0 to 5 deg is commanded. For both cases, coupling between lateral and longitudinal axes is expected due to the inertia cross-coupling and gravity terms in the nonlinear aircraft equations of motion. The inertia coupling between lateral and longitudinal axes is evident from the pitch angle transient. Coupling into pitch angle is very small. For both cases, there are some initial overshoot and oscillation. However, these dissipate completely within 5 s. Better response quality is expected with servo lag and a realistic command time history, such as a ramp instead of a step input. This is attributed to the strong coupling between yaw and roll axes. In Fig. 6c, note that there is a large rudder deflection for the sideslip demand. This is due to loss of rudder effectiveness at low-dynamic pressure or high-sideslip-angle demand. Cross coupling has remained small in either case. For all of the simulations, the controller action is rapid. All control deflections are found to stay within an acceptable deflection angle.

The significant improvement resulting from the ramp input is evident in Fig. 7a for a roll angle demand from 0 to 50 deg. This is nearly a 2-g turn maneuver. Coupling between lateral and longitudinal axes can be seen easily in Fig. 7a. The steady-state value of the angle of attack is 6.5 deg. Also, there is a large deflection of elevator to increase the lift. For this maneuver, the controller action exhibits some chatter, probably due to numerical errors.

IV. Conclusions

We have shown that a nonlinear system with PI controller can be translated into a singular perturbation problem. A new control system design method using a multivariable high-gain, error-actuated analog controller is used for the design of approximate noninteracting control law for nonlinear systems. This design scheme is applied to the design of a decoupling flight control law for the full aircraft model.

This example shows that output-feedback solutions from the linear case satisfy the required conditions, i.e., stabilizing and decoupling, for application to nonlinear systems. The resulting nonlinear closed-loop systems exhibit approximate noninteracting behavior when operated in a neighborhood of the family of constant operating points. These results confirm that a satisfactory controller for nonlinear systems can be designed by the proposed method. Again, it is emphasized that this stabilizing and near decoupling result is achieved by using a PI output feedback controller. Also, this design method is readily applicable to an unstable system as demonstrated.

The results also show the feasibility of a constant gain output feedback, with the advantage of reducing implementation complexity, by reducing the number of costly sensors. Reliability is also improved because there are fewer sensors.

References

[1]Falb, P. L., and Wolovich, W. A., "Decoupling in the Design and Synthesis of Multivariable Control Systems," *IEEE Transactions on Automatic Control*, Vol. AC-12, No. 12, 1967, pp. 651–659.

[2]Morse, S. A., and Wonham, W. M., "Status of Noninteracting Control," *IEEE Transactions on Automatic Control*, Vol. AC-16, No. 12, 1971, pp. 568–581.

[3]Singh, S. N., and Rugh, W. J., "Decoupling in a Class of Nonlinear Systems by State Variable Feedback," *Journal of Dynamic Systems, Measurement and Control*, Vol. 94, 1972, pp. 323–329.

[4]Isidori, A., and Grizzle, J. W., "Fixed Modes and Nonlinear Noninteracting Control with Stability," *IEEE Transactions on Automatic Control*, Vol. AC-32, No. 10, 1988, pp. 907–914.

[5]Isidori, A., Krener, A. J., Gori-Giorgi, C., and Monaco, S., "Nonlinear Decoupling via Feedback: A Differential Geometric Approach," *IEEE Transactions on Automatic Control*, Vol. AC-26, No. 2, 1981, pp. 331–345.

[6]Gras, L., and Nijmeijer, H., "Decoupling in Nonlinear Systems: from Linearity to Nonlinearity," *IEE Proceedings*, Vol. 136, Pt. D, No. 2, 1989, pp. 53–62.

[7]Park, S., "Decoupled Flight Control System Design Using the Singular Perturbation Method," Ph.D. Dissertation, Dept. of Aerospace Engineering, Wichita State Univ., Wichita, KS, Nov. 1992.

[8]Kokotovic, P. V., Khalil, H. K., and O'Reilly, J., *Singular Perturbation Methods in Control: Analysis and Design*, Academic, New York, 1981.

[9]Kokotovic, P. V., O'Malley, R. E., and Sanuti, P., "Singular Perturbations and Order Reduction in Control Theory: An Overview," *Automatica*, Vol. 12, No. 2, 1976, pp. 123–132.

[10]Porter, B., and Shenton, A. T., "Singular Perturbation Analysis of the Transfer Function Matrices of a Class of Multivariable Linear Systems," *International Journal of Control*, Vol. 21, No. 4, 1975, pp. 655–660.

[11]Porter, B., and Bradshaw, A., "Singular Perturbation Methods in the Design of Tracking Systems Incorporating Inner-Loop Compensators and High-Gain Error-Actuated Controllers," *International Journal of Systems Science*, Vol. 12, No. 10, 1981, pp. 1193–1205.

[12]Porter, B., and Bradshaw, A., "Singular Perturbation Methods in the Design of Tracking Systems Incorporating Inner-Loop Compensators and Fast-Sampling Error–Actuated Controllers," *International Journal of Systems Science*, Vol. 12, Oct. 1981, pp. 1207–1220.

[13]Roskam, J., "Airplane Flight Dynamics and Automatic Flight Control," Roskam Aviation and Engineering Corp., Ottawa, KS, 1979, pp. 616–619.